Journal of Computational Physics **157,** 302–326 (2000)
doi:10.1006/jcph.1999.6379, available online at http://www.idealibrary.com on IDEAL®

Simplified Discretization of Systems of Hyperbolic Conservation Laws Containing Advection Equations

Ronald P. Fedkiw, Barry Merriman, and Stanley Osher[1]

Department of Mathematics, University of California at Los Angeles, 405 Hilgard Avenue, Los Angeles, California 90095-1555

Received April 6, 1998; revised August 30, 1999

The high speed flow of complex materials can often be modeled by the compressible Euler equations coupled to (possibly many) additional advection equations. Traditionally, good computational results have been obtained by writing these systems in fully conservative form and applying the general methodology of shock-capturing schemes for systems of hyperbolic conservation laws. In this paper, we show how to obtain the benefits of these schemes without the usual complexity of full characteristic decomposition or the restrictions imposed by fully conservative differencing. Instead, under certain conditions defined in Section 2, the additional advection equations can be discretized individually with a nonconservative scheme while the remaining system is discretized using a fully conservative approach, perhaps based on a characteristic field decomposition. A simple extension of the Lax–Wendroff Theorem is presented to show that under certain verifiable hypothesis, our nonconservative schemes converge to weak solutions of the fully conservative system. Then this new technique is applied to systems of equations from compressible multiphase flow, chemically reacting flow, and explosive materials modeling. In the last instance, the flexibility introduced by this approach is exploited to change a weakly hyperbolic system into an equivalent strictly hyperbolic system, and to remove certain nonphysical modeling assumptions.

1. INTRODUCTION

It is widely believed that numerical methods for discretizing the Euler equations should have discrete conservation of mass, momentum, and energy as well as an entropy fix for low viscosity schemes. Conservative schemes have limit solutions which are weak solutions of the Euler equations yielding accurate representation of the shock speeds and jumps. In

[1]Research supported in part by ONR N00014-97-1-0027, ONR N00014-97-1-0968.

0021-9991/00 $35.00

contrast, nonconservative schemes generally give limit solutions which have incorrect shock speeds and/or jumps, e.g., see [15]. Note that the work in [13] derived and used special viscosity terms that mimic the Navier–Stokes viscosity in order to reduce these types of nonconservative errors.

As models become richer in physics and mathematics, more and more equations are added. Some common examples are the addition of mass fraction equations for chemically reacting flow [7] and the addition of the level set equation for compressible gas flow [18]. Another example is the Baer–Nunziato (BN) two phase model for solid explosives and propellants [1], where a second set of Euler equations is added for the solid phase, and a volume fraction equation is added to close the system. In addition, the chemical source terms of the BN model require the addition of many more equations, not all of which are known or agreed upon by the community [10, 2]. As new conservation laws are added to the Euler equations, the Jacobian matrix required for upwind schemes grows accordingly, usually becoming large and unwieldy.

For a given system one can often identify a minimal conservative system that contains the truly nonlinear fields. In the chemically reacting flow model and the level set model the Euler equations are the minimal system containing the sound waves. It will be shown that both the mass fraction equations and the level set equation can be written in advection form and upwinded separately according to the particle velocity without degrading the quality of the numerical solution. In fact, the resulting solution is as good, if not better than the fully conservative method. In the BN model, the minimal conservative system consists of the two sets of Euler equations which contain the truly nonlinear fields for both the gas sound waves and the solid sound waves. The volume fraction equation and the extra equations added for chemical source terms will be put into advection form and upwinded separately according to the appropriate particle velocity (gas or solid). Note that the BN system differs from the first two examples, where the minimal system was only the Euler equations and all added equations were put into advection form. The reason for this difference is that the second set of Euler equations, added to model the solid, contains quantities which have jumps that are not advected along streamlines, e.g., shock waves in the solid.

One often adds new advection equations of the form

$$Z_t + uZ_x = 0 \tag{1}$$

to the minimal system. The continuity equation is

$$\rho_t + (\rho u)_x = 0, \tag{2}$$

where ρ is the density and u is the velocity. Multiplying Eq. (1) by ρ and adding it to Z times Eq. (2) results in

$$(\rho Z)_t + (\rho Z u)_x = 0 \tag{3}$$

as a new equation in conservation form. If the correct Rankine–Hugoniot jump conditions of the full system are such that discontinuities in Z are advected along streamlines then the technique introduced in this paper applies. This is the case for the mass fraction equations, the level set equation, and the volume fraction equation of the BN model, but not the case for the second set of Euler equations in the BN model which must be added to the minimal system. As a further illustration, consider

$$S_t + uS_x = 0, \tag{4}$$

where S is the entropy per unit mass. While this equation is valid away from shocks, discontinuities in S are not necessarily advected along streamlines and the technique introduced in this paper does not apply. The advection of discontinuities in Z along streamlines can be made more precise by considering a discontinuity moving with speed D. The well known jump conditions for Eqs. (2) and (3) are

$$\rho_{left}(u_{left} - D) = \rho_{right}(u_{right} - D) \tag{5}$$

and

$$\rho_{left} Z_{left}(u_{left} - D) = \rho_{right} Z_{right}(u_{right} - D) \tag{6}$$

which can be combined to obtain

$$\rho_{right}(Z_{left} - Z_{right})(u_{right} - D) = 0 \tag{7}$$

illustrating that Z must be continuous, unless $u_{right} = D = u_{left}$. That is, discontinuities of Z move with the particle velocity. Moreover Z is continuous across shocks. Note that these statements are generally not true for the entropy.

There are two distinct kinds of advection equations which may be added to a minimal system. The first kind advects quantities that the minimal system depends on; examples include dependence of the pressure on the mass fractions, the level set function, or the volume fraction. The left and right eigenvectors of the Jacobian matrix are needed in order to use an upwind scheme. These types of advection equations dictate an increase in the size of the left eigenvector, since information is needed from these variables to accurately project into the characteristic fields. However, the right eigenvector remains the length of the minimal system, since only the minimal system is updated using the characteristic fields, while the advection equations are updated individually. The second kind of advection equation advects those quantities that the minimal system does *not* depend on, even though the new equations may be dependent on the minimal system for their characteristic velocity. These types of equations occur in newer models such as the BN equations where the advected quantities have been added in order to model the chemical source terms. These advection equations have no effect on the hyperbolic part of the minimal system and do not change the eigensystem at all, i.e., neither the right nor left eigenvector of the associated Jacobian matrix of the minimal system changes. Here the savings in simplicity of scheme design and programming effort are enormous using our technique rather than standard conservation form discretizations, because one only needs to discretize simple additional advection equations. There are also significant gains in execution time.

In Section 5, a conservative equation that introduces a weak hyperbolicity in the BN model (which implies that the problem is mildly ill-posed) is discussed. In this instance, the identification of a quantity with discontinuities that advect along streamlines is extremely useful since the conservative equation is equivalent to advecting a quantity which blows up analytically as the reaction proceeds to completion. This problem is easily fixed by advecting an equivalent quantity which goes to zero as the reaction proceeds to completion. Furthermore, putting this well behaved advection equation into conservative form and solving in the usual way removes the weak hyperbolicity for the full conservation form as well.

Once the advection equations are isolated from the minimal conservative system, greater flexibility in scheme design can be exploited. If the advected quantity is continuous, e.g., the

level set function, then one can use high order essentially nonoscillatory (ENO) Hamilton–Jacobi methods which gain an order of accuracy at extrema over the conservative ENO flux method and are also somewhat easier to implement [21, 11]. If the advected quantity is discontinuous, our theoretical and numerical results indicate that nonconservative flux form is preferable. That is, we recommend that the spatial term of

$$Z_t + uZ_x = 0 \tag{8}$$

be approximated as

$$uZ_x \approx u_i \frac{\left(\hat{Z}_{i+\frac{1}{2}} - \hat{Z}_{i-\frac{1}{2}}\right)}{\Delta x}, \tag{9}$$

where $\hat{Z}_{i+1/2}$ can be viewed as a numerical flux function consistent with Z. For discontinuous advected quantities, the contact discontinuities can be sharpened with artificial compression methods [22]. In fact, isolating the advection equations in a flux form that allows nonconservative flux differencing opens up new research avenues such as the pursuit of a fully multidimensional artificial compression method, which could not be carried out as easily with conservative numerical methods.

2. THEORETICAL JUSTIFICATION

The general theorem concerns the following system of equations in $R^3 \times R^+$

$$q_t + \nabla \cdot \mathbf{f}(q, Z) = 0 \tag{10}$$

$$Z_t + \mathbf{u} \cdot \nabla Z = 0, \tag{11}$$

where $\mathbf{f} = (f, g, h)$ and $\mathbf{u} = (u, v, w)$. Note that q, f, g, and h are all l vectors while Z is an m vector. In regions of smoothness, we assume that Eqs. (10) and (11) are equivalent to a conservative system having $l + m$ dependent variables and that the jump conditions for the conservative system are

$$[\mathbf{f} \cdot \mathbf{N}] = D[q] \tag{12}$$

$$[Z](\mathbf{u} \cdot \mathbf{N} - D) = 0, \tag{13}$$

where $\mathbf{N}$ is the unit normal to the surface of discontinuity, and D is the local discontinuity speed in the normal direction. For simplicity of exposition only we consider $R^2 \times R^+$ in the following.

We approximate the system using the conservation form for the q variables and the nonconservative flux based form for the Z variables. Thus we have

$$q_{i,j}^{n+1} = q_{i,j}^n - \frac{\Delta t}{\Delta x}\left[\left(F_{i+\frac{1}{2},j}^n - F_{i-\frac{1}{2},j}^n\right) + \left(G_{i,j+\frac{1}{2}}^n - G_{i,j-\frac{1}{2}}^n\right)\right], \tag{14}$$

where $F_{i\pm1/2,j}^n$ and $G_{i,j\pm1/2}^n$ are Lipschitz continuous numerical flux functions consistent with $f(q, Z)$ and $g(q, Z)$, respectively. We also have

$$Z_{i,j}^{n+1} = Z_{i,j}^n - \frac{\Delta t}{\Delta x}\left[u_{i,j}^n\left(\hat{Z}_{i+\frac{1}{2},j}^n - \hat{Z}_{i-\frac{1}{2},j}^n\right) + v_{i,j}^n\left(\hat{Z}_{i,j+\frac{1}{2}} - \hat{Z}_{i,j-\frac{1}{2}}\right)\right], \tag{15}$$

where $\hat{Z}_{i\pm1/2,j}^n$ and $\hat{Z}_{i,j\pm1/2}^n$ are Lipschitz continuous flux functions consistent with Z.

We make the following assumptions: Suppose, as $\Delta t, \Delta x, \Delta y \to 0$, a subsequence of the approximate solutions generated by Eqs. (14) and (15) is bounded a.e. convergent to a piecewise differentiable limit, (q, Z), for which Z has jumps only where $\mathbf{u}$ is differentiable. In addition we assume that the first divided differences in x and y of these approximations $u^n_{i,j}$ and $v^n_{i,j}$ are uniformly bounded by an integrable function in any compact set $\Omega \subset R^2$ for which the limit solution (u, v) is differentiable, i.e., $u^n_{i,j}$ and $v^n_{i,j}$ are each uniformly bounded in $W^{1,1}(\Omega)$, and that similar statements are true for $Z^n_{i,j}$ in any compact set $\Omega' \subset R^2$ for which the limit solution Z is differentiable. Then we have the following result:

THEOREM 1. *The piecewise differentiable limit* (q, Z) *is a weak solution of Eqs.* (10) *and* (11), *i.e., it is a classical solution when it is differentiable and it satisfies Eqs.* (12) *and* (13) *at jumps.*

Remark 1. Our assumptions are considerably stronger than those of the classical Lax–Wendroff theorem [14] which requires only bounded a.e. convergence. Nevertheless, in our calculations in this paper (and elsewhere) using this method, we have observed that our assumptions were valid. In fact the divided differences of the approximations to $\mathbf{u}$ were always uniformly bounded away from the discontinuities of the limiting $\mathbf{u}$ in our calculations, and similarly for Z.

Remark 2. The content of our theorem is along the lines: convergence plus consistency implies the limit solution satisfies the original differential equation. Here, this amounts to showing that the jump conditions in Eqs. (12) and (13) are satisfied and that Eqs. (10) and (11) are true in regions of smoothness.

Remark 3. The Lax–Wendroff Theorem states that a converged solution is a weak solution. Thus one has to believe their results have or will converge with further grid refinement. Our theorem requires this as well as the requirement that Z has jumps only where $\mathbf{u}$ is differentiable and that the approximations to $\mathbf{u}$ are uniformly bounded in $W^{1,1}$ wherever $\mathbf{u}$ is differentiable, with similar requirements on Z and its approximations. One has to believe that no singularities will appear and violate these hypothesis as the grid is refined. This is in the spirit of the Lax–Wendroff Theorem, i.e., if it has not happened on the finest computational grid (lack of apparent convergence, or in our case, singularities in the wrong places), then one can quote the appropriate theorem to justify convergence.

Remark 4. For an arbitrary system of conservation laws to have the decomposition in Eqs. (10) to (13), it is necessary that one of the eigenvalues of the Jacobian matrix in each dimension be (u, v, w), respectively, each repeated at least m times. This is, of course, only a necessary condition.

Remark 5. Our main theorem may appear to contradict some prevailing wisdom. For example, in [16] the authors state that the advection Eq. (11) "does not hold a priori across a shock." This is, of course, generally true, but we have proven that it does hold in our sense if Z remains continuous there.

Proof. Let $\varphi(x, y, t)$ be a $C^1_0(R^2 \times R^+)$ function. We multiply Eqs. (14) and (15) by $\varphi(x_i, y_j, t^n)$ and use the summation-by-parts idea in the proof of the LW theorem, arriving

at

$$\sum_{i,j,n} \Delta t \Delta x \Delta y \left[q^n_{i,j} \left(\frac{\varphi(x_i, y_j, t^n) - \varphi(x_i, y_j, t^{n-1})}{\Delta t} \right) + F^n_{i+\frac{1}{2},j} \left(\frac{\varphi(x_{i+1}, y_j, t^n) - \varphi(x_i, y_j, t^n)}{\Delta x} \right) + G^n_{i,j+\frac{1}{2}} \left(\frac{\varphi(x_i, y_{j+1}, t^n) - \varphi(x_i, y_j, t^n)}{\Delta y} \right) \right] = 0 \tag{16}$$

and

$$\sum_{i,j,n} \Delta t \Delta x \Delta y \left[Z^n_{i,j} \left(\frac{\varphi(x_i, y_j, t^n) - \varphi(x_i, y_j, t^{n-1})}{\Delta t} \right) + \hat{Z}^n_{i+\frac{1}{2},j} \left(\frac{u^n_{i+1,j} \varphi(x_{i+1}, y_j, t^n) - u^n_{i,j} \varphi(x_i, y_j, t^n)}{\Delta x} \right) + \hat{Z}^n_{i,j+\frac{1}{2}} \left(\frac{v^n_{i,j+1} \varphi(x_i, y_{j+1}, t^n) - v^n_{i,j} \varphi(x_i, y_j, t^n)}{\Delta y} \right) \right] = 0. \tag{17}$$

We let $\Delta t, \Delta x, \Delta y \to 0$ for the converging subsequence. From Eq. (16), exactly as in the proof of the Lax–Wendroff theorem (which uses the Lebesgue dominated convergence theorem, the Lipschitz continuity of the flux functions, consistency, and the fact that

$$\lim_{h \to 0} \nu(x + h) = \nu(x) \tag{18}$$

a.e. for bounded measurable functions ν), we have

$$\int_{R^2 \times R^+} q\varphi_t + f\varphi_z + g\varphi_y = 0 \tag{19}$$

for any such test function φ. This, of course, implies that q is a classical solution of Eq. (10) wherever q and Z are smooth and that q and Z satisfy Eq. (12) at jumps.

Next we use the identity

$$\frac{u^n_{i+1,j} \varphi(x_{i+1}, y_j, t^n) - u^n_{i,j} \varphi(x_i, y_j, t^n)}{\Delta x} = u^n_{i+1,j} \left(\frac{\varphi(x_{i+1}, y_j, t^n) - \varphi(x_i, y_j, t^n)}{\Delta x} \right) + \left(\frac{u^n_{i+1,j} - u^n_{i,j}}{\Delta x} \right) \varphi(x_i, y_j, t^n) \tag{20}$$

and the analogous identity involving y divided differences. Choose φ to have support in a region Ω in which $\mathbf{u}$ is differentiable. We let $\Delta x, \Delta y, \Delta t \to 0$ along the converging subsequence. Using Eqs. (17) and (20), the Lebesgue dominated convergence theorem and the usual Lax–Wendroff argument we arrive at

$$\int_{R^2 \times R^+} Z\varphi_t + Z(\mathbf{u} \cdot \nabla \varphi) + Z(\nabla \cdot \mathbf{u})\varphi = 0. \tag{21}$$

If Z is differentiable in Ω, a simple integration by parts gives us

$$\int_{\Omega} \varphi(Z_t + \mathbf{u} \cdot \nabla Z) = 0 \tag{22}$$

for any such φ, hence Z is a classical solution of (11) in Ω. If Z has a jump we take Ω to be a sphere centered at a point of discontinuity. We then let the radius of the sphere go to zero in Eq. (21) and obtain the jump conditions in Eq. (13) in a standard fashion.

We may prove Z is a classical solution when u jumps with the help of the dominated convergence theorem arriving at Eq. (22) in a straightforward fashion.

3. LEVEL SET EQUATION FOR COMPRESSIBLE FLOW

Consider the one-dimensional Euler equations with the level set equation in conservation form

$$\begin{pmatrix} \rho \\ \rho u \\ E \\ \rho\phi \end{pmatrix}_t + \begin{pmatrix} \rho_u \\ \rho u^2 + p \\ (E+p)u \\ \rho u \phi \end{pmatrix}_x = 0, \tag{23}$$

where ρ is the density, u is the velocity, E is the total energy per unit volume, p is the pressure, and ϕ is the level set function. Another alternative, as suggested in [18], is to replace the conservative level set equation (4th equation) with the level set equation in quasilinear or advection form

$$\phi_t + u\phi_x = 0 \tag{24}$$

noting that ϕ is valid in advection form since the values of ϕ are meant to advect with the particle velocity u, i.e., along streamlines.

3.1. *Projection into Characteristic Fields*

Modern shock capturing schemes are often based on projection into characteristic fields. Usually the value of the left eigenvector of the Jacobian matrix is frozen and used to locally decompose the system. Consider the Euler equations with the level set equation in advection form. Projection by a left eigenvector, $L = (l_1, l_2, l_3, l_4)$, leads to

$$\left[(l_1, l_2, l_3, l_4) \begin{pmatrix} \rho \\ \rho u \\ E \\ \phi \end{pmatrix} \right]_t + \left[(l_1, l_2, l_3) \begin{pmatrix} \rho u \\ \rho u^2 + p \\ (E+p)u \end{pmatrix} \right]_x + l_4 u \phi_x = 0, \tag{25}$$

where it is obvious that the spatial part of this equation cannot be written in conservation form. In order to obtain conservation form for the projected equation one needs to use the conservative version of the level set equation so that projection by a left eigenvector leads to

$$\left[(l_1, l_2, l_3, l_4) \begin{pmatrix} \rho \\ \rho u \\ E \\ \rho\phi \end{pmatrix} \right]_t + \left[(l_1, l_2, l_3, l_4) \begin{pmatrix} \rho u \\ \rho u^2 + p \\ (E+p)u \\ \rho u \phi \end{pmatrix} \right]_x = 0 \tag{26}$$

in conservation form. For this reason, the level set equation is written in conservation form when formulating the Jacobian matrix and the associated eigensystem.

3.2. *Conservative Eigensystem*

The total energy is the sum of the internal energy and the kinetic energy,

$$E = \rho e + \frac{\rho u^2}{2}, \tag{27}$$

where e is the internal energy per unit mass. The pressure can be written as $p = p(\rho, e, \phi)$ with partial derivatives p_ρ, p_e, and p_ϕ. Alternatively, considering the pressure as $p = p(\rho, \rho u, E, \rho\phi)$ allows one to write the partial derivatives of the pressure with respect to the conserved variables as

$$\frac{\partial p}{\partial \rho} = \hat{H} - \frac{\phi p_\phi}{\rho}, \qquad \hat{H} = c^2 - \Gamma(H - u^2) \tag{28}$$

$$\frac{\partial p}{\partial (\rho u)} = -\Gamma u, \qquad \frac{\partial p}{\partial E} = \Gamma \tag{29}$$

$$\frac{\partial p}{\partial (\rho\phi)} = \frac{p_\phi}{\rho}, \tag{30}$$

where the Gruneisen coefficient, the sound speed, and the total mixture enthalpy are defined by

$$\Gamma = \frac{p_e}{\rho}, \qquad c = \sqrt{p_\rho + \frac{\Gamma p}{\rho}} \tag{31}$$

$$H = \frac{E + p}{\rho}. \tag{32}$$

The partial derivatives of the pressure are used to obtain the Jacobian matrix

$$\begin{pmatrix} 0 & 1 & 0 & 0 \\ -u^2 + \hat{H} - \frac{\phi p_\phi}{\rho} & 2u - \Gamma u & \Gamma & \frac{p_\phi}{\rho} \\ -uH + u\hat{H} - \frac{u\phi p_\phi}{\rho} & H - \Gamma u^2 & u + \Gamma u & \frac{u p_\phi}{\rho} \\ -u\phi & \phi & 0 & u \end{pmatrix} \tag{33}$$

and the associated eigensystem

$$\mathbf{R}^1 = \begin{pmatrix} 1 \\ u - c \\ H - uc \\ \phi \end{pmatrix}, \qquad \mathbf{R}^2 = \begin{pmatrix} 1 \\ u \\ H - \frac{1}{b_1} \\ \phi \end{pmatrix} \tag{34}$$

$$\mathbf{R}^3 = \begin{pmatrix} 1 \\ u + c \\ H + uc \\ \phi \end{pmatrix}, \qquad \mathbf{R}^4 = \begin{pmatrix} 0 \\ 0 \\ -\frac{p_\phi}{\Gamma \rho} \\ 1 \end{pmatrix} \tag{35}$$

$$\mathbf{L}^1 = \left(\frac{b_2}{2} + \frac{u}{2c} - \frac{\phi p_\phi}{2\rho c^2}, \frac{-b_1 u}{2} - \frac{1}{2c}, \frac{b_1}{2}, \frac{p_\phi}{2\rho c^2} \right) \tag{36}$$

$$\mathbf{L}^2 = \left(1 - b_2 + \frac{\phi p_\phi}{\rho c^2}, b_1 u, -b_1, -\frac{p_\phi}{\rho c^2}\right) \tag{37}$$

$$\mathbf{L}^3 = \left(\frac{b_2}{2} - \frac{u}{2c} - \frac{\phi p_\phi}{2\rho c^2}, \frac{-b_1 u}{2} + \frac{1}{2c}, \frac{b_1}{2}, \frac{p_\phi}{2\rho c^2}\right) \tag{38}$$

$$\mathbf{L}^4 = (-\phi, 0, 0, 1), \tag{39}$$

where

$$b_1 = \frac{p_e}{\rho c^2}, \qquad b_2 = 1 + b_1 u^2 - b_1 H. \tag{40}$$

3.3. *Numerical Method*

When discretizing along the lines of [22], the left eigenvectors are used to project into the characteristic fields, the scalar flux in each characteristic field is discretized based on the associated eigenvalue in that field, and the right eigenvectors are used to project out of the characteristic fields. Then the contributions from each characteristic field are added together to produce the total vector flux at a cell interface. These vector fluxes are differenced in the usual manner resulting in a fully conservative numerical method.

In order to correctly project into the characteristic fields, the full left eigenvector is always used. However, since conservation form is not required for the last equation, i.e., the level set equation, only the first three components of the right eigenvectors are used to project out of the characteristic fields. The level set equation is discretized independently in advection form, noting that its characteristic information is determined by u and that nothing about it need be conserved.

Consider the Ghost Fluid Method, developed in [5], where p_ϕ is identically zero. The minimal system no longer depends on the level set equation and only the first three components of the first three left and right eigenvectors are needed to update the minimal system. That is, the one dimensional Euler equations can be discretized with a standard conservative scheme while the level set equation is independently discretized in advection form. For both one- and two-dimensional computational results along with comparisons to the exact solutions, see [5].

4. CHEMICALLY REACTING FLOW

Consider the two-dimensional thermally perfect Euler equations for multi-species flow with a total of N species,

$$\mathbf{U}_t + [\mathbf{F}(\mathbf{U})]_x + [\mathbf{G}(\mathbf{U})]_y = 0, \tag{41}$$

$$\mathbf{U} = \begin{pmatrix} \rho \\ \rho u \\ \rho v \\ E \\ \rho Y_1 \\ \vdots \\ \rho Y_{N-1} \end{pmatrix}, \qquad \mathbf{F}(\mathbf{U}) = \begin{pmatrix} \rho u \\ \rho u^2 + p \\ \rho uv \\ (E+p)u \\ \rho u Y_1 \\ \vdots \\ \rho u Y_{N-1} \end{pmatrix}, \qquad \mathbf{G}(\mathbf{U}) = \begin{pmatrix} \rho v \\ \rho uv \\ \rho v^2 + p \\ (E+p)v \\ \rho v Y_1 \\ \vdots \\ \rho v Y_{N-1}, \end{pmatrix} \tag{42}$$

$$E = -p + \frac{\rho(u^2+v^2)}{2} + \rho\left(\sum_{i=1}^{n} Y_i h_i\right), \qquad h_i(T) = h_i^f + \int_0^T c_{p,i}(s)\,ds, \quad (43)$$

where t is time, x and y are the spatial dimensions, ρ is the density, u and v are the velocities, E is the energy per unit volume, Y_i is the mass fraction of species i, h_i is the enthalpy per unit mass of species i, h_i^f is the heat of formation of species i (enthalpy at $0\,K$), $c_{p,i}$ is the specific heat at constant pressure of species i, and p is the pressure [7]. Note that $Y_N = 1 - \sum_{i=1}^{N-1} Y_i$. The pressure is a function of the density, internal energy per unit mass, and the mass fractions, $p = p(\rho, e, Y_1, \ldots, Y_{N-1})$, with partial derivatives p_ρ, p_e and p_{Y_i} where $E = \rho e + \rho(u^2+v^2)/2$ defines the internal energy per unit mass.

The eigenvalues and eigenvectors for the Jacobian matrix of $\mathbf{F}(\mathbf{U})$ are obtained by setting $A=1$ and $B=0$ in the following formulas, while those for the Jacobian matrix of $\mathbf{G}(\mathbf{U})$ are obtained by setting $A=0$ and $B=1$.

The eigenvalues are

$$\lambda^1 = \hat{u} - c, \qquad \lambda^{N+3} = \hat{u} + c \quad (44)$$

$$\lambda^2 = \cdots = \lambda^{N+2} = \hat{u}, \quad (45)$$

where $\hat{u}$ is repeated $(N+1)$ times.

The standard construction of upwind difference schemes requires the full eigensystem of the Jacobian matrix of $\mathbf{F}$ evaluated as some intermediate value of $\mathbf{U}$. When this Jacobian matrix has a repeated eigenvalue, this involves finding a basis for the associated eigenspace which can be complicated for systems with high multiplicity. The complementary projection method (CPM) is an alternative approach where full upwinding is accomplished without the use of the eigenvectors in the repeated eigenvalue field. Suppose the first p eigenvalues are repeated, then the corresponding p dimensional characteristic subspace is the span of $(\mathbf{L}^1, \ldots, \mathbf{L}^p)$. The remaining left and right eigenvectors can be used to define

$$f^K = \mathbf{L}^K \cdot \mathbf{F} \quad (46)$$

and write

$$\mathbf{F} = \boldsymbol{\mathcal{F}} + \sum_{k=p+1}^{n} f^K \mathbf{R}^K, \quad (47)$$

where the vector $\boldsymbol{\mathcal{F}}$ can be upwinded according to the sign of the repeated eigenvalue $\lambda^1 = \lambda^2 \ldots = \lambda^p$, and no basis need be chosen for $\boldsymbol{\mathcal{F}}$. For more details on the CPM, see [6].

The CPM requires the first and $(N+3)$rd left and right eigenvectors for the chemically reacting flow example considered here. In addition, since the minimal conservative system is the two-dimensional Euler equations, only the first four entries of the right eigenvectors are needed. The necessary left and right eigenvectors are

$$\mathbf{L}^1 = \left(\frac{b_2}{2} + \frac{\hat{u}}{2c} + \frac{b_3}{2}, -\frac{b_1 u}{2} - \frac{A}{2c}, -\frac{b_1 v}{2} - \frac{B}{2c}, \frac{b_1}{2}, \frac{-b_1 z_1}{2}, \ldots, \frac{-b_1 z_{N-1}}{2}\right) \quad (48)$$

$$\mathbf{L}^{N+3} = \left(\frac{b_2}{2} - \frac{\hat{u}}{2c} + \frac{b_3}{2}, -\frac{b_1 u}{2} + \frac{A}{2c}, -\frac{b_1 v}{2} + \frac{B}{2c}, \frac{b_1}{2}, \frac{-b_1 z_1}{2}, \ldots, \frac{-b_1 z_{N-1}}{2}\right) \quad (49)$$

$$\mathbf{R}^1 = \begin{pmatrix} 1 \\ u - Ac \\ v - Bc \\ H - \hat{u}c \end{pmatrix}, \qquad \mathbf{R}^{N+3} = \begin{pmatrix} 1 \\ u + Ac \\ v + Bc \\ H + \hat{u}c \end{pmatrix}, \quad (50)$$

where the unnecessary terms in the right eigenvectors have been omitted for brevity and

$$q^2 = u^2 + v^2, \qquad \hat{u} = Au + Bv \tag{51}$$

$$c = \sqrt{p_\rho + \frac{pp_e}{\rho^2}}, \qquad H = \frac{E+p}{\rho}, \tag{52}$$

$$b_1 = \frac{p_e}{\rho c^2}, \qquad b_2 = 1 + b_1 q^2 - b_1 H, \tag{53}$$

$$b_3 = b_1 \sum_{i=1}^{N-1} Y_i z_i, \qquad z_i = \frac{-p_{Y_i}}{p_e}. \tag{54}$$

4.1. *Numerical Method*

The two left eigenvectors are used to project into the two nonlinear fields, while only the first four entries of the right eigenvectors are used to project out of these fields. The CPM is used to construct the complementary subspace

$$\mathcal{F} = \begin{pmatrix} \rho u \\ \rho u^2 + p \\ \rho uv \\ (E+p)u \end{pmatrix} - \mathbf{L}^1\mathbf{F}(\mathbf{U})\mathbf{R}^1 - \mathbf{L}^{N+3}\mathbf{F}(\mathbf{U})\mathbf{R}^{N+3}, \tag{55}$$

where $\mathcal{F}$ has length four and each of its component can be upwind differenced in the upwind direction determined by u. The resulting flux is combined with the flux contributions from the two nonlinear fields to yield the net numerical flux for the first four entries of $\mathbf{F}(\mathbf{U})$. These fluxes are differenced in the usual manner to get the proper upwind conservative discretization for the first four equations, i.e., for the minimal system. For a dimension by dimension discretization, the same procedure is applied to the flux in the other spatial dimension, and then the total spatial contribution can be used with a TVD Runge Kutta method to update the first four equations of the system, i.e., to update the minimal system. The advection equations for the mass fractions

$$\begin{pmatrix} Y_1 \\ \vdots \\ Y_{N-1} \end{pmatrix}_t + u \begin{pmatrix} Y_1 \\ \vdots \\ Y_{N-1} \end{pmatrix}_x + v \begin{pmatrix} Y_1 \\ \vdots \\ Y_{N-1,} \end{pmatrix}_y = 0 \tag{56}$$

are discretized independently in an equation by equation fashion noting that the characteristic information for the x and y derivatives is determined by u and v, respectively, and that nothing need be conserved.

4.2. *Examples*

Several of the examples from [4, 7] were recomputed using the nonconservative flux based method outlined in this paper. Overall, the calculations using the new technique agreed well with the old calculations. One particularly difficult example from [7] is repeated here.

Consider a 0.12 m domain with a shock wave located a $x = 0.06$ m traveling from right to left in a 2/1/7 molar ratio of $H_2/O_2/Ar$ where all gases are assumed to be thermally perfect and a full chemical reaction mechanism is employed as discussed in [7]. The initial data for the shock wave consist of $\rho = .072\ \frac{\text{kg}}{\text{m}^3}$, $u = 0\ \frac{\text{m}}{\text{s}}$ and $p = 7173$ Pa on the left with

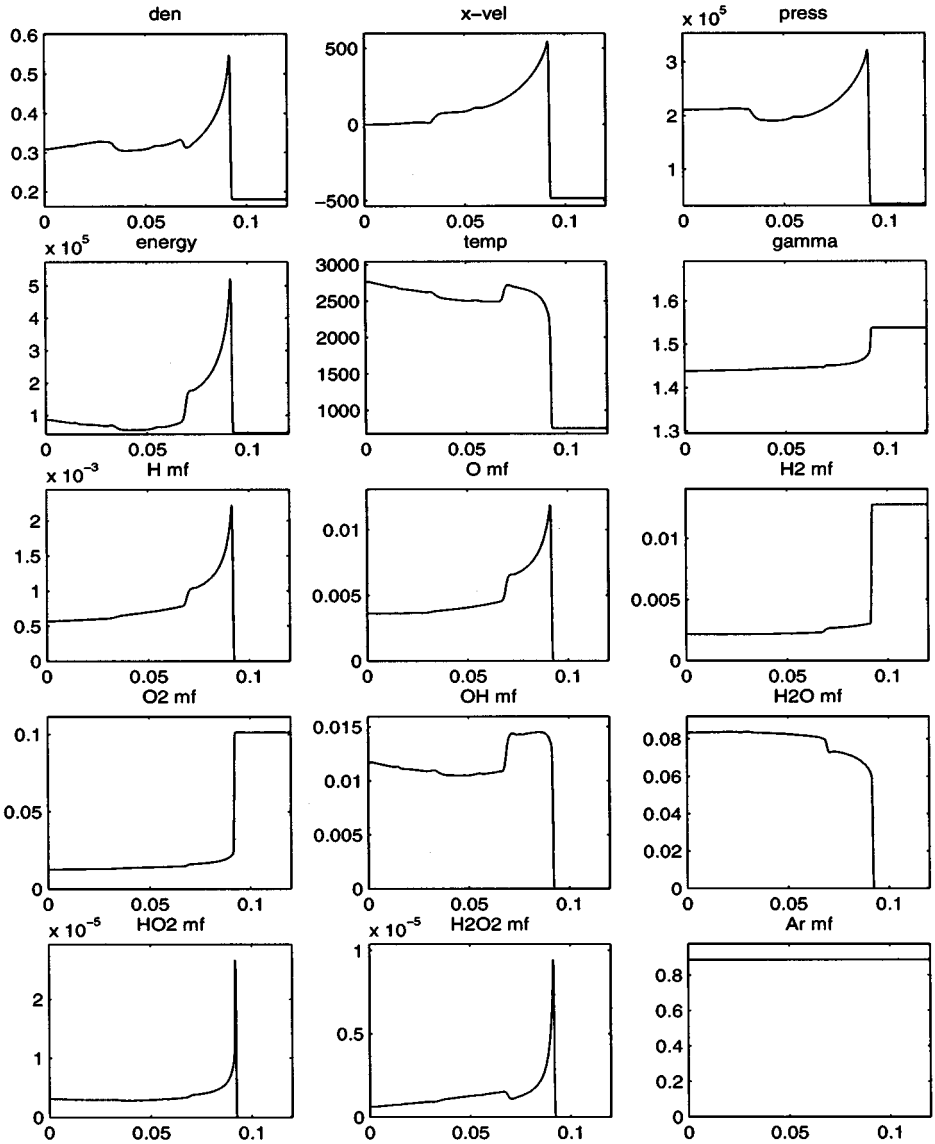

FIG. 1. Fully conservative method.

$\rho = .18075\ \frac{\text{kg}}{\text{m}^3}$, $u = -487.34\ \frac{\text{m}}{\text{s}}$, and $p = 35594$ Pa on the right. A solid wall boundary condition is applied at $x = 0$ m and the shock wave reflects off this wall changing its direction of travel. As this shock wave passes over the gas a second time, the gas is heated enough to initiate chemical reactions. After a suitable induction time, a chemical combustion wave forms at the wall and travels to the right eventually overtaking the shock wave resulting in the formation of three waves. From left to right, there is a rarefaction wave, a contact discontinuity, and a detonation wave.

Figure 1 shows the solution at 230 μs with 400 uniform grid cells and 2300 equal time steps using the fully conservative ENO-RF method outlined in [7]. Figure 2 shows the same calculation using the nonconservative flux based ENO method (outlined in the Appendix) for the mass fraction equations. The CPM [6] was used in both calculations. In [7], this was shown to be a very sensitive problem, and the good agreement of the two methods is

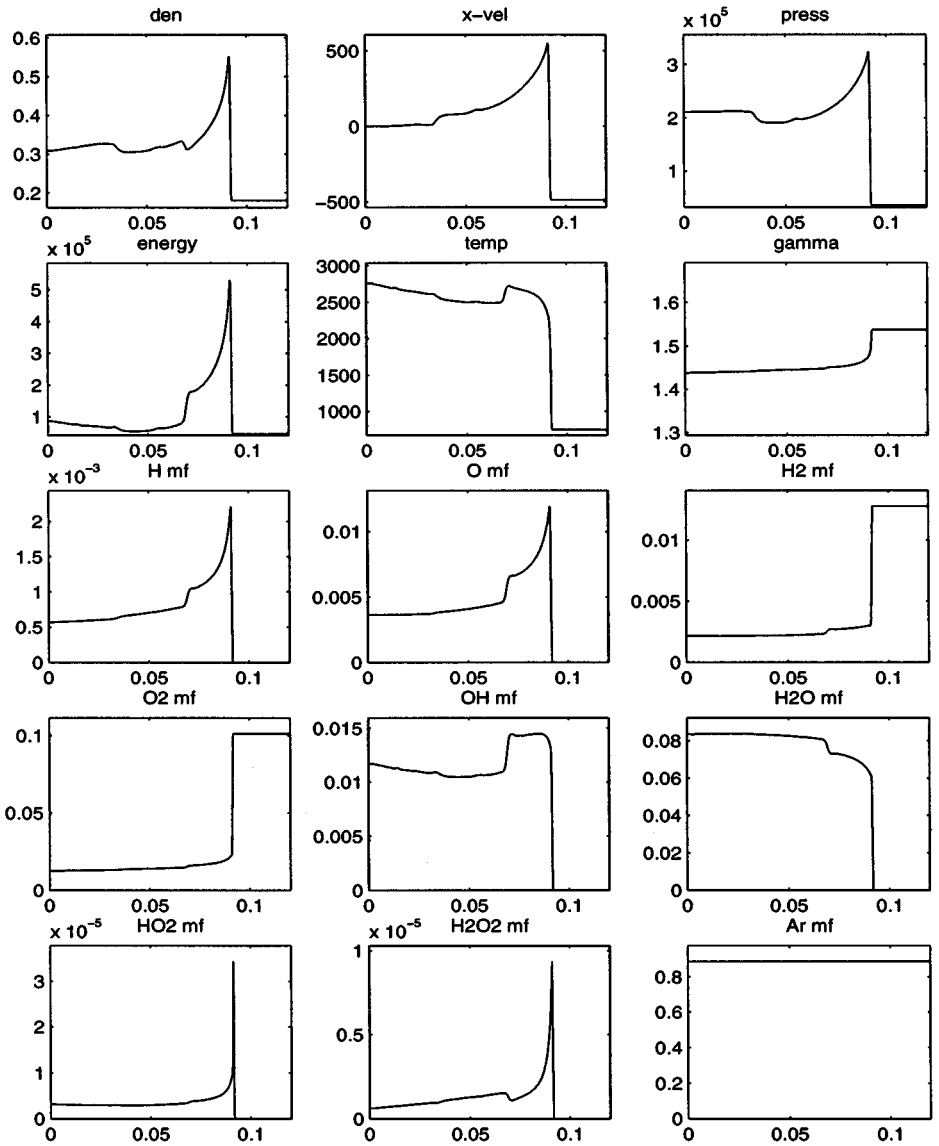

FIG. 2. Nonconservative flux based algorithm.

promising. The only major difference is in the height of the HO_2 peak, although this seems to have no effect on the rest of the solution.

A grid refinement study was carried out with 100, 200, 400, 800, and 1600 grid cells using 575, 1150, 2300, 4600, and 9200 time steps, respectively. Figure 3 shows the results with the fully conservative scheme while Fig. 4 shows the results with the nonconservative flux based method for the mass fraction equations. The position of the lead detonation wave converges with first order accuracy for both numerical algorithms. In addition, the peaks in the HO_2 mass fraction seem to converge more uniformly (i.e., monotonically) for the nonconservative flux based method. Figures 5, 6, and 7 compare the two methods with 100, 400, and 1600 grid points, respectively. The fully conservative method is plotted with *x*'s while the nonconservative flux based method is plotted with *o*'s.

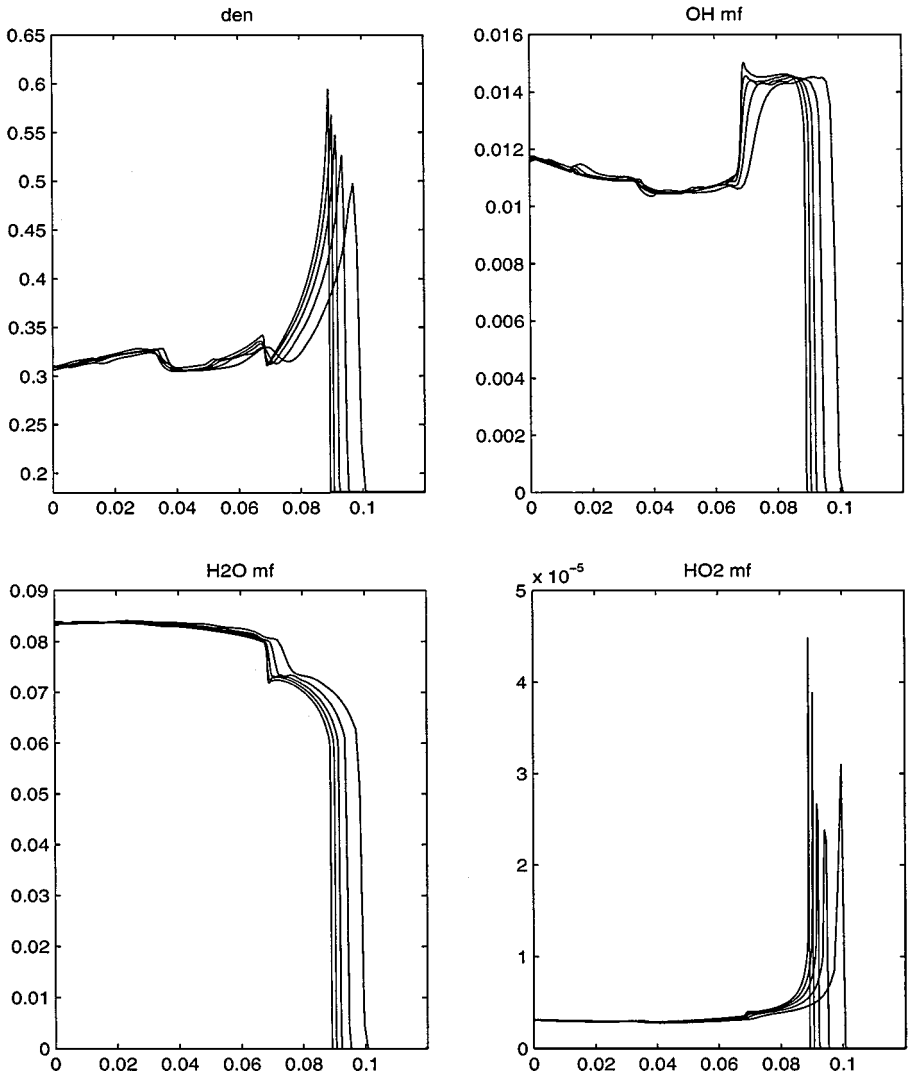

FIG. 3. Fully conservative method.

5. BN TWO PHASE EXPLOSIVES MODEL

Consider a simplified version of the one-dimensional Baer–Nunziato (BN) two phase explosives model [1, 3, 10, 2] that ignores nozzling and source terms

$$\begin{pmatrix} \rho_g\phi_g \\ \rho_g u_g\phi_g \\ E_g\phi_g \\ \rho_s\phi_s \\ \rho_s u_s\phi_s \\ E_s\phi_s \\ \rho_s \end{pmatrix}_t + \begin{pmatrix} \rho_g u_g\phi_g \\ \left(\rho_g u_g^2 + p_g\right)\phi_g \\ (E_g + p_g)u_g\phi_g \\ \rho_s u_s\phi_s \\ \left(\rho_s u_s^2 + p_s\right)\phi_s \\ (E_s + p_s)u_s\phi_s \\ \rho_s u_s \end{pmatrix}_x = 0, \tag{57}$$

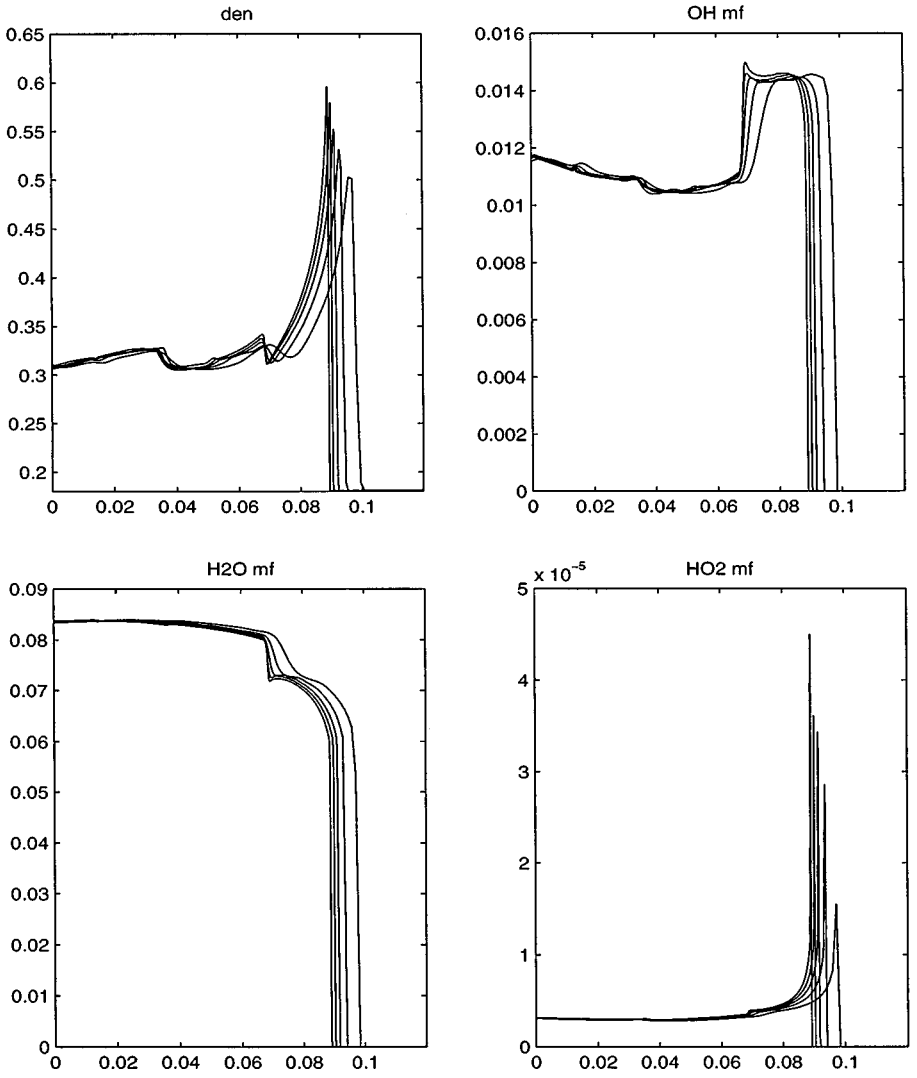

FIG. 4. Nonconservative flux based algorithm.

where t is time, x is the spatial dimension, ρ_g, u_g, E_g, p_g, and ϕ_g are the density, velocity, energy per unit volume, pressure, and volume fraction of the gas, and ρ_s, u_s, E_s, p_s, and ϕ_s are the density, velocity, energy per unit volume, pressure, and volume fraction of the solid. The seventh equation is the compaction equation which is used to close the system along with the saturation condition, $\phi_s + \phi_g = 1$. Assuming that neither phase has any material strength, the pressure of each phase is a function of the density and internal energy per unit mass of that phase, $p_g = p_g(\rho_g, e_g)$ and $p_s = p_s(\rho_s, e_s)$, with partial derivatives $(p_s)_{\rho_s}$, $(p_s)_{e_s}$, $(p_g)_{\rho_g}$, and $(p_g)_{e_g}$ where $E_g = \rho_g e_g + \rho_g u_g^2/2$ and $E_s = \rho_s e_s + \rho_s u_s^2/2$ define the internal energies per unit mass. In addition, assume that the equations of state are defined in a manner consistent with $(p_g)_{\rho_g} = p_g/\rho_g$ and $(p_s)_{\rho_s} = p_s/\rho_s$ as identities. A more detailed version of the model is considered in [8].

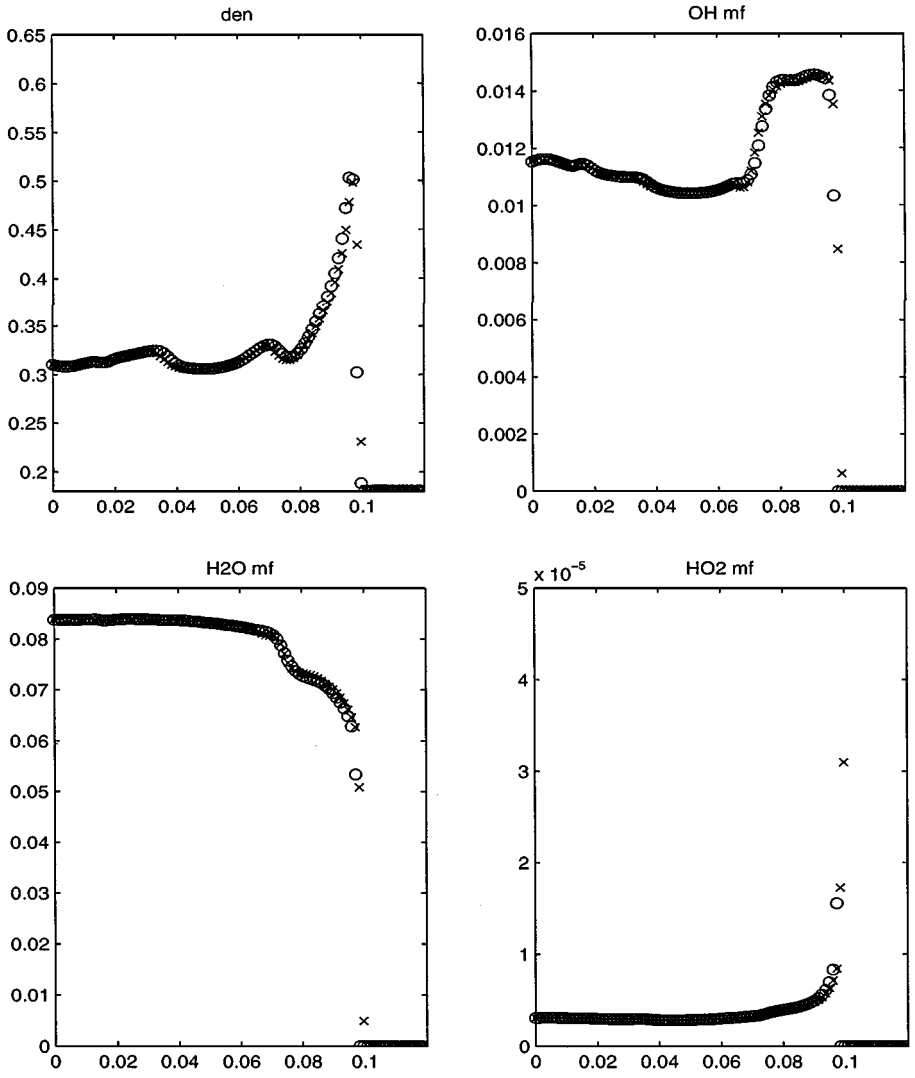

FIG. 5. The 100 grid cells; ×, conservative; ○, nonconservative.

Under the above assumptions, the eigenvalues are $u_g - c_g$, u_g, $u_g + c_g$, $u_s - c_s$, u_s, $u_s + c_s$, and u_s, with corresponding left and right eigenvectors

$$\mathbf{L}^1 = \left(\frac{b_{2g}}{2} + \frac{u_g}{2c_g}, \frac{-b_{1g}u_g}{2} - \frac{1}{2c_g}, \frac{b_{1g}}{2}, 0, 0, 0, 0\right) \tag{58}$$

$$\mathbf{L}^2 = \left(1 - b_{2g}, b_{1g}u_g, -b_{1g}, 0, 0, 0, 0\right) \tag{59}$$

$$\mathbf{L}^3 = \left(\frac{b_{2g}}{2} - \frac{u_g}{2c_g}, \frac{-b_{1g}u_g}{2} + \frac{1}{2c_g}, \frac{b_{1g}}{2}, 0, 0, 0, 0\right) \tag{60}$$

$$\mathbf{L}^4 = \left(0, 0, 0, \frac{b_{2s}}{2} + \frac{u_s}{2c_s}, \frac{-b_{1s}u_s}{2} - \frac{1}{2c_s}, \frac{b_{1s}}{2}, 0\right) \tag{61}$$

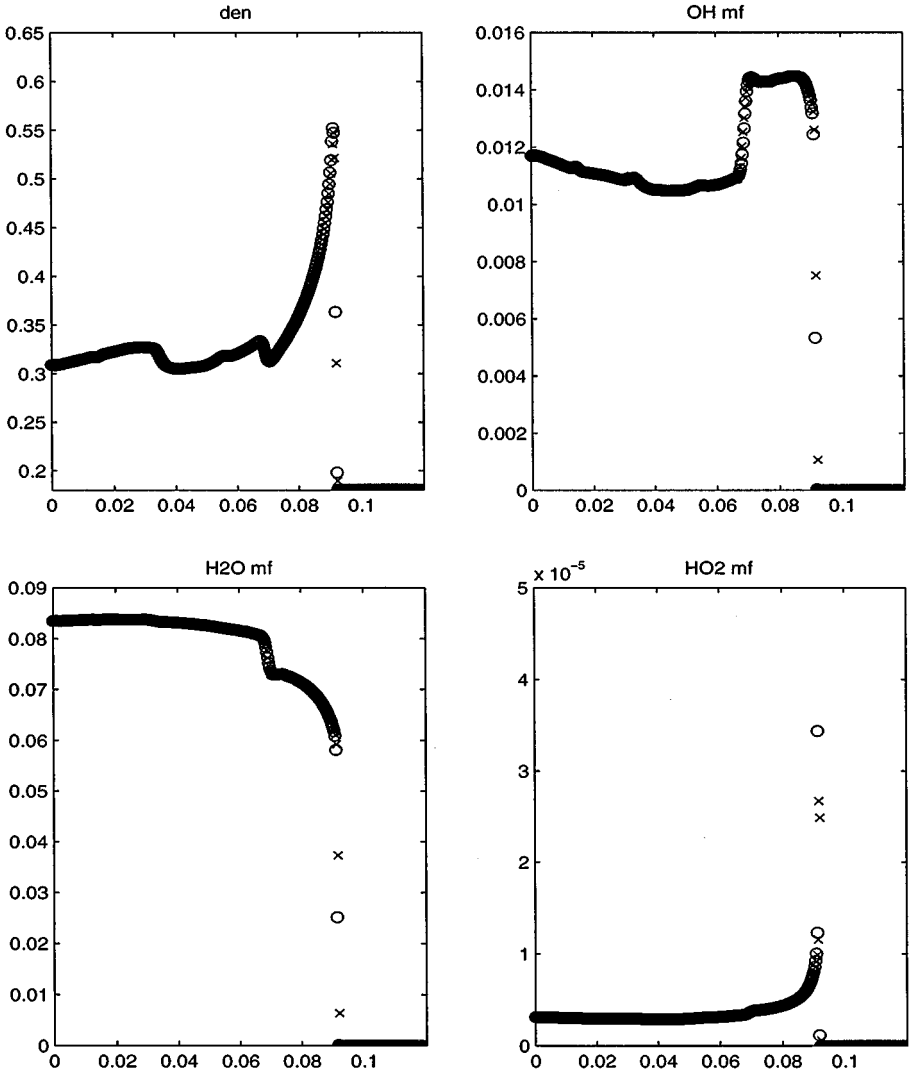

FIG. 6. The 400 grid cells; ×, conservative; ○, nonconservative.

$$\mathbf{L}^5 = (0, 0, 0, 1 - b_{2s}, b_{1s}u_s, -b_{1s}, 0) \tag{62}$$

$$\mathbf{L}^6 = \left(0, 0, 0, \frac{b_{2s}}{2} - \frac{u_s}{2c_s}, \frac{-b_{1s}u_s}{2} + \frac{1}{2c_s}, \frac{b_{1s}}{2}, 0\right) \tag{63}$$

$$\mathbf{L}^7 = (0, 0, 0, -1, 0, 0, \phi_s) \tag{64}$$

$$\mathbf{R}^1 = \begin{pmatrix} 1 \\ u_g - c_g \\ H_g - u_g c_g \\ 0 \\ 0 \\ 0 \\ 0 \end{pmatrix}, \quad \mathbf{R}^2 = \begin{pmatrix} 1 \\ u_g \\ H_g - \frac{1}{b_{1g}} \\ 0 \\ 0 \\ 0 \\ 0 \end{pmatrix}, \quad \mathbf{R}^3 = \begin{pmatrix} 1 \\ u_g + c_g \\ H_g + u_g c_g \\ 0 \\ 0 \\ 0 \\ 0 \end{pmatrix} \tag{65}$$

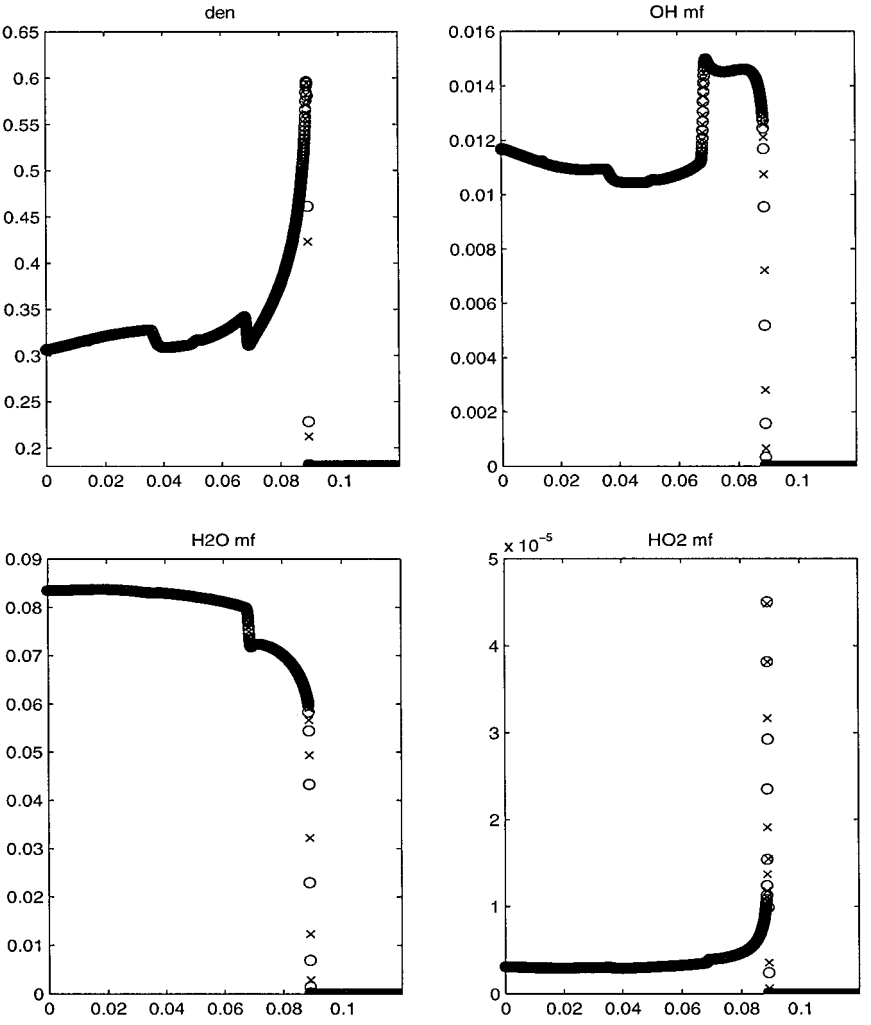

FIG. 7. The 1600 grid cells; ×, conservative; ○, nonconservative.

$$\mathbf{R}^4 = \begin{pmatrix} 0 \\ 0 \\ 0 \\ 1 \\ u_s - c_s \\ H_s - u_s c_s \\ \frac{1}{\phi_s} \end{pmatrix}, \qquad \mathbf{R}^5 = \begin{pmatrix} 0 \\ 0 \\ 0 \\ 1 \\ u_s \\ H_s - \frac{1}{b_{1s}} \\ \frac{1}{\phi_s} \end{pmatrix}, \qquad \mathbf{R}^6 = \begin{pmatrix} 0 \\ 0 \\ 0 \\ 1 \\ u_s + c_s \\ H_s + u_s c_s \\ \frac{1}{\phi_s} \end{pmatrix} \tag{66}$$

$$\mathbf{R}^7 = \begin{pmatrix} 0 \\ 0 \\ 0 \\ 0 \\ 0 \\ 0 \\ \frac{1}{\phi_s} \end{pmatrix} \tag{67}$$

$$\Gamma_g = \frac{(p_g)_{e_g}}{\rho_g}, \qquad c_g = \sqrt{(p_g)_{\rho_g} + \frac{\Gamma_g p_g}{\rho_g}} \tag{68}$$

$$\Gamma_s = \frac{(p_s)_{e_s}}{\rho_s}, \qquad c_s = \sqrt{(p_s)_{\rho_s} + \frac{\Gamma_s p_s}{\rho_s}} \tag{69}$$

$$H_g = \frac{E_g + p_g}{\rho_g}, \qquad H_s = \frac{E_s + p_s}{\rho_s} \tag{70}$$

$$b_{1g} = \frac{\Gamma_g}{c_g^2}, \qquad b_{2g} = 1 + b_{1g}u_g^2 - b_{1g}H_g \tag{71}$$

$$b_{1s} = \frac{\Gamma_s}{c_s^2}, \qquad b_{2s} = 1 + b_{1s}u_s^2 - b_{1s}H_s. \tag{72}$$

5.1. *Numerical Method*

The seven left eigenvectors are used to project into the characteristic fields, while only the first six entries of the seven right eigenvectors are used to project out of these fields, since the minimal system consists of the first six equations. This avoids the common division by zero problem introduced by the seventh term in the right eigenvectors, i.e., the $1/\phi_s$ term. This term blows up when a chemical reaction depletes ϕ_s to zero and has forced unphysical modeling, e.g., solid cores [10], to avoid the problem. (Another method used to avoid this problem involves the use of central schemes [17, 19].) In [8], a priori knowledge that the seventh entry of the right eigenvectors could be discarded motivated manipulation of the eigensystem in a manner that forces this division by zero problem into that location eliminating it entirely.

The volume fraction evolution equation

$$(\phi_s)_t + u_s(\phi_s)_x = 0 \tag{73}$$

is an advection equation, and it can be discretized independently noting that the characteristic information is determined by u_s and that nothing need be conserved.

5.2. *Examples*

In [10], a conservation law for the number of particles per unit volume

$$n_t + (u_s n)_x = 0 \tag{74}$$

was added to the one-dimensional BN model. Inclusion of Eq. (74) leads to a new weak hyperbolicity when $\phi_s = 0$ due to the "blow-up" of the resulting $n/\rho_s\phi_s$ term in the eigensystem. See [10] for details.

Using the continuity equation for the solid, Eq. (74) can be rewritten in advection form

$$\left(\frac{n}{\rho_s\phi_s}\right)_t + u_s\left(\frac{n}{\rho_s\phi_s}\right)_x = 0, \tag{75}$$

where the advected quantity is the number or particles per unit mass. This quantity blows up as the chemical reaction proceeds to completion, i.e., as $\phi_s \to 0$. Since n is defined as

the volume fraction divided by the particle volume

$$n = \frac{\phi_s}{V_p} \tag{76}$$

Eq. (75) is equivalent to

$$\left(\frac{1}{\rho_s V_p}\right)_t + u_s \left(\frac{1}{\rho_s V_p}\right)_x = 0 \tag{77}$$

which blows up when $V_p \to 0$.

The problem with Eqs. (74), (75), and (77) is that they are all derived by advecting a quantity that blows up as the reaction proceeds to completion. This can trivially be avoided by advecting an equivalent quantity that vanishes as the reaction proceeds to completion. As the number of particles per unit mass blows up, the mass per particle vanishes. Replacing Eq. (75) with

$$(\rho_s V_p)_t + u_s (\rho_s V_p)_x = 0 \tag{78}$$

and solving this equation in advection form removes the weak hyperbolicity. All that remains are some decoding errors that occur when computing n from Eq. (76), although n is no longer needed to solve the system. If conservation form is preferred, then Eq. (78) can be combined with the continuity equation of the solid to obtain

$$\left(\rho_s^2 \phi_s V_p\right)_t + \left(u_s \rho_s^2 \phi_s V_p\right)_x = 0 \tag{79}$$

which can be substituted in place of Eq. (74) resulting in an eigensystem that contains a well behaved $\rho_s V_p$ term instead of a poorly behaved $n/\rho_s \phi_s$ term.

In Fig. 8 we repeat a simple shock tube calculation from [10] using Eq. (78) for the mass per particle to replace the conservation equation for n. We use a 10 m domain with 200 grid cells and a final time of 0.006 s. Initially, $\rho_g = \rho_s = 10 \frac{\text{kg}}{\text{m}^3}$ and $p_g = p_s = 1.0 \times 10^6$ Pa on the left, while $\rho_g = \rho_s = 1 \frac{\text{kg}}{\text{m}^3}$ and $p_g = p_s = 1.0 \times 10^5$ Pa on the right. In addition, $u_g = u_s = 0 \frac{\text{m}}{\text{s}}$, $\phi_s = 0.7$, and $n = 1.19 \times 10^{11} \frac{\text{particles}}{\text{m}^3}$ everywhere. Both the solid and the gas phase are assumed to obey $p = \rho RT$ and $e = c_v T$ with $R_g = R_s = 287 \frac{\text{J}}{\text{kgK}}$, $(c_v)_g = 718 \frac{\text{J}}{\text{kgK}}$, and $(c_v)_s = 239 \frac{\text{J}}{\text{kgK}}$. The results compare well with those from [10] where the conservation equation for n was used. Note that the solution for the mass per particle variable only contains a simple contact discontinuity propagating to the right, while the solutions for the particle volume variable and the number of particle per unit volume variable both contain shocks and rarefactions.

APPENDIX A: CENTRAL SCHEMES

The examples in this paper were discussed based on an upwind discretization with eigenvector projections. In this appendix, a central discretization is briefly discussed. See [17, 19] for examples of central schemes.

Consider the one-dimensional Euler equations with Z satisfying the following advection equation

$$Z_t + u Z_x = 0 \tag{80}$$

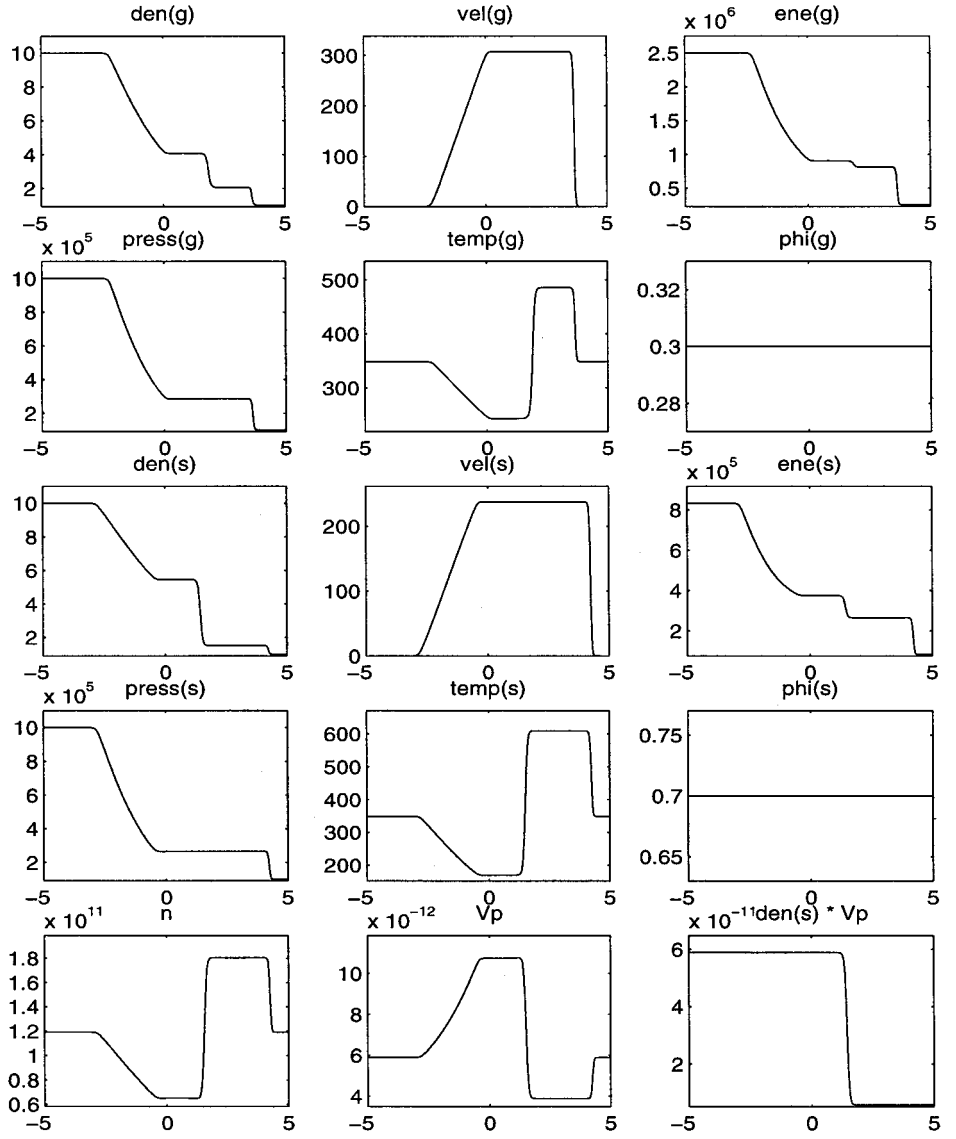

FIG. 8. BN calculation.

which can be placed into conservation form along with the Euler equations

$$\begin{pmatrix} \rho \\ \rho u \\ E \\ \rho Z \end{pmatrix}_t + \begin{pmatrix} \rho u \\ \rho u^2 + p \\ (E+p)u \\ \rho u Z \end{pmatrix}_x = 0 \tag{81}$$

and discretized equation by equation with a central scheme. The new technique presented in this paper would not alter the central discretization of the Euler equations, but Eq. (80) would be discretized in nonconservative form instead of

$$(\rho Z)_t + (\rho u Z)_x = 0 \tag{82}$$

in conservation form. Equation (82) requires artificial numerical dissipation proportional to the maximum of $|u+c|$ and $|u-c|$ when discretizing with a central scheme since it includes the continuity equation by construction. Moreover, shocks and rarefactions can occur in ρZ. In contrast, Eq. (80) does not require this (possibly large) numerical dissipation and there are no shocks or rarefactions in Z.

APPENDIX B: ADVECTION EQUATION DISCRETIZATION

Consider an advection equation of the form

$$Z_t + uZ_x + vZ_y = 0, \tag{83}$$

where Z is the advected quantity and u and v are the particle velocities in the x and y direction, respectively. Nonconservative flux based discretizations for Z_x are given below. Z_y is discretized in a similar fashion and then these two terms are combined with u and v at each grid node before applying a 3rd order TVD Runge Kutta method [9, 22] for time integration.

B.1. *Nonconservative Flux Based ENO Discretization*

A nonconservative extension of the ENO-Roe discretization is used, since there are no nonlinear waves such as shocks and rarefactions [9, 22].

The numerical flux function F is defined through the relation

$$(Z_x)_i = \frac{F_{i+\frac{1}{2}} - F_{i-\frac{1}{2}}}{\Delta x}, \tag{84}$$

where the $F_{i\pm 1/2}$ are the values of the numerical flux function at the cell walls. The numerical flux function is constructed at the cell walls by considering the primitive function H of another function h, where h is identical to the numerical flux function F at the cell walls.

H is calculated at the cell walls with polynomial interpolation. The zeroth order divided differences, $D^0_{i+1/2}$, and all higher order *even* divided differences of H exist at the cell walls and have the subscript $i \pm \frac{1}{2}$. The first order divided differences D^1_i and all higher order *odd* divided differences of H exist at the grid points and have the subscript i. Note that the zeroth order divided differences of H vanish with differentiation and are not needed.

The first order divided differences of H are

$$D^1_i H = Z_i \tag{85}$$

and the higher divided differences are

$$D^2_{i+\frac{1}{2}} H = \frac{1}{2} D^1_{i+\frac{1}{2}} Z, \qquad D^3_i H = \frac{1}{3} D^2_i Z. \tag{86}$$

Consider a specific grid point i_0. If $u_{i_0} = 0$, then setting $(Z_x)_{i_0} = 0$ will be algorithmically correct since $(uZ_x)_{i_0} = 0$ is desired, otherwise u_{i_0} determines the upwind direction.

The associated numerical flux function $F_{i_0+1/2}$ is defined as follows: If $u_{i_0} > 0$, then $k = i_0$. If $u_{i_0} < 0$, then $k = i_0 + 1$. Define

$$Q_1(x) = \left(D^1_k H\right)\left(x - x_{i_0+\frac{1}{2}}\right). \tag{87}$$

If $|D^2_{k-1/2}H| \le |D^2_{k+1/2}H|$, then $c = D^2_{k-1/2}H$ and $k^\star = k-1$. Otherwise, $c = D^2_{k+1/2}H$ and $k^\star = k$. Define

$$Q_2(x) = c\left(x - x_{k-\frac{1}{2}}\right)\left(x - x_{k+\frac{1}{2}}\right). \tag{88}$$

If $|D^3_{k^\star}H| \le |D^3_{k^\star+1}H|$, then $c^\star = D^3_{k^\star}H$. Otherwise, $c^\star = D^3_{k^\star+1}H$. Define

$$Q_3(x) = c^\star\left(x - x_{k^\star-\frac{1}{2}}\right)\left(x - x_{k^\star+\frac{1}{2}}\right)\left(x - x_{k^\star+\frac{3}{2}}\right). \tag{89}$$

Then

$$F_{i_0+\frac{1}{2}} = D^1_k H + c(2(i_0-k)+1)\Delta x + c^\star\left(3(i_0-k^\star)^2 - 1\right)(\Delta x)^2. \tag{90}$$

Likewise, the associated numerical flux function $F_{i_0-1/2}$ is defined as follows: If $u_{i_0} > 0$, then $k = i_0 - 1$. If $u_{i_0} < 0$, then $k = i_0$. Define

$$Q_1(x) = \left(D^1_k H\right)\left(x - x_{i_0-\frac{1}{2}}\right). \tag{91}$$

If $|D^2_{k-1/2}H| \le |D^2_{k+1/2}H|$, then $c = D^2_{k-1/2}H$ and $k^\star = k-1$. Otherwise, $c = D^2_{k+1/2}H$ and $k^\star = k$. Define

$$Q_2(x) = c\left(x - x_{k-\frac{1}{2}}\right)\left(x - x_{k+\frac{1}{2}}\right). \tag{92}$$

If $|D^3_{k^\star}H||D^3_{k^\star+1}H|$, then $c^\star = D^3_{k^\star}H$. Otherwise, $c^\star = D^3_{k^\star+1}H$. Define

$$Q_3(x) = c^\star\left(x - x_{k^\star-\frac{1}{2}}\right)\left(x - x_{k^\star+\frac{1}{2}}\right)\left(x - x_{k^\star+\frac{3}{2}}\right). \tag{93}$$

Then

$$F_{i_0-\frac{1}{2}} = D^1_k H + c(2(i_0-1-k)+1)\Delta x + c^\star(3(i_0-1-k^\star)^2 - 1)(\Delta x)^2. \tag{94}$$

Finally, $(Z_x)_{i_0}$ is given by Eq. (84).

B.2. *Nonconservative Flux Based WENO Discretization*

Consider a 5th order WENO scheme with the parameter ϵ [12]. Large values of ϵ cause the stencil to be biased toward central differencing (causing oscillations), while small values of ϵ cause the stencil to be biased toward 3rd order ENO (lowering the order). To get a stencil biased toward the fifth order flux ϵ is defined as

$$\epsilon = 10^{-6}\max\left\{v_1^2, v_2^2, v_3^2, v_4^2, v_5^2\right\} + 10^{-99}, \tag{95}$$

where 10^{-99} is used to avoid division by zero and should be much smaller than the first term in most regions of the domain.

Consider a specific grid point i_0. If $u_{i_0} = 0$, then setting $(Z_x)_{i_0} = 0$ will be algorithmically correct since $(uZ_x)_{i_0} = 0$ is desired, otherwise u_{i_0} determines the upwind direction.

The associated numerical flux function $F_{i_0+1/2}$ is defined as follows: If $u_{i_0} > 0$, then $v_1 = Z_{i_0-2}$, $v_2 = Z_{i_0-1}$, $v_3 = Z_{i_0}$, $v_4 = Z_{i_0+1}$, and $v_5 = Z_{i_0+2}$. If $u_{i_0} < 0$, then $v_1 = Z_{i_0+3}$, $v_2 = Z_{i_0+2}$, $v_3 = Z_{i_0+1}$, $v_4 = Z_{i_0}$, and $v_5 = Z_{i_0-1}$.

Define the smoothness

$$S_1 = \frac{13}{12}(v_1 - 2v_2 + v_3)^2 + \frac{1}{4}(v_1 - 4v_2 + 3v_3)^2 \tag{96}$$

$$S_2 = \frac{13}{12}(v_2 - 2v_3 + v_4)^2 + \frac{1}{4}(v_4 - v_4)^2 \tag{97}$$

$$S_3 = \frac{13}{12}(v_3 - 2v_4 + v_5)^2 + \frac{1}{4}(3v_3 - 4v_4 + v_5)^2 \tag{98}$$

and the weights

$$a_1 = \frac{1}{10}\frac{1}{(\epsilon + S_1)^2}, \qquad w_1 = \frac{a_1}{a_1 + a_2 + a_3} \tag{99}$$

$$a_2 = \frac{6}{10}\frac{1}{(\epsilon + S_2)^2}, \qquad w_2 = \frac{a_2}{a_2 + a_2 + a_3} \tag{100}$$

$$a_3 = \frac{3}{10}\frac{1}{(\epsilon + S_3)^2}, \qquad w_3 = \frac{a_3}{a_3 + a_2 + a_3} \tag{101}$$

to get the flux

$$F_{i_0+\frac{1}{2}} = w_1\left(\frac{v_1}{3} - \frac{7v_2}{6} + \frac{11v_3}{6}\right) + w_2\left(\frac{-v_2}{6} + \frac{5v_3}{6} + \frac{v_4}{3}\right) + w_3\left(\frac{v_3}{3} + \frac{5v_4}{6} - \frac{v_5}{6}\right). \tag{102}$$

Likewise, the associated numerical flux function $F_{i_0-1/2}$ is defined as follows: If $u_{i_0} > 0$, then $v_1 = Z_{i_0-3}$, $v_2 = Z_{i_0-2}$, $v_3 = Z_{i_0-1}$, $v_4 = Z_{i_0}$, and $v_5 = Z_{i_0+1}$. If $u_{i_0} < 0$, then $v_1 = Z_{i_0+2}$, $v_2 = Z_{i_0+1}$, $v_3 = Z_{i_0}$, $v_4 = Z_{i_0-1}$, and $v_5 = Z_{i_0-2}$.

Then the smoothness, weights, and flux are defined exactly as above yielding

$$F_{i_0-\frac{1}{2}} = w_1\left(\frac{v_1}{3} - \frac{7v_2}{6} + \frac{11v_3}{6}\right) + w_2\left(\frac{-v_2}{6} + \frac{5v_3}{6} + \frac{v_4}{3}\right) + w_3\left(\frac{v_3}{3} + \frac{5v_4}{6} - \frac{v_5}{6}\right). \tag{103}$$

Finally,

$$(Z_x)_{i_0} = \frac{F_{i_0+\frac{1}{2}} - F_{i_0-\frac{1}{2}}}{\Delta x}. \tag{104}$$

REFERENCES

1. M. Baer and J. Nunziato, A two-phase mixture theory for the the deflagration to detonation transition (DDT) in reactive granular materials, *Int. J. Multiphase Flow* **12**(6), 861 (1986).
2. J. B. Bdzil, R. Menikoff, S. F. Son, A. K. Kapila, and D. S. Stewart, Two-phase modeling of deflagration-to-detonation transition in granular materials: A critical examination of modeling issues, *Phys. Fluids* **11**, 378 (1999).
3. J. B. Bdzil and S. F. Son, *Engineering Models of Deflagration to Detonation Transition*, LA-12794-MS, 1994.
4. R. P. Fedkiw, *A Survey of Chemically Reacting, Compressible Flows*, Dissertation, UCLA, 1996.

5. R. Fedkiw, T. Aslam, B. Merriman, and S. Osher, A non-oscillatory Eulerian approach to interfaces in multimaterial flows (The ghost fluid method), *J. Comput. Phys*. **152**, 457 (1999).
6. R. Fedkiw, B. Merriman, and S. Osher, Efficient characteristic projection in upwind difference schemes for hyperbolic systems (The complementary projection method), *J. Comput. Phys*. **141**, 22 (1998).
7. R. Fedkiw, B. Merriman, and S. Osher, High accuracy numerical methods for thermally perfect gas flows with chemistry, *J. Comput. Phys*. **132**, 175 (1997).
8. R. Fedkiw, B. Merriman, and S. Osher, A high order efficient numerical approach to the BN two phase explosives model, in preparation.
9. R. Fedkiw, B. Merriman, R. Donat, and S. Osher, The penultimate scheme for systems of conservation laws: Finite difference ENO with Marquina's flux splitting, in *Progress in Numerical Solutions of Partial Differential Equations, Arachon, France*, edited by M. Hafez (July 1998).
10. K. A. Gonthier, *A Numerical Investigation of the Evolution of Self-Propagating Detonation in Energetic Granular Solids*, Dissertation, University of Notre Dame, 1996.
11. G.-S. Jiang and D. Peng, Weighted ENO schemes for Hamilton Jacobi equations, *SIAM J. Numer. Anal*., in press.
12. G.-S. Jiang and C.-W. Shu, Efficient implementation of weighted ENO schemes, *J. Comput. Phys*. **126**, 202 (1996).
13. S. Karni, Viscous shock profiles and primitive formulations, *SIAM J. Numer. Anal*. **29**, 1592 (1992).
14. P. D. Lax and B. Wendroff, Systems of conservation laws, *Comm. Pure Appl. Math*. **13**, 217 (1960).
15. R. J. Leveque, *Numerical Methods for Conservation Laws* (Birkäuser-Verlag, Basel, 1992), p. 123.
16. B. Larrouturou and L. Fezoui, On the equations of multi-component perfect of real gas inviscid flow, in Lecture Notes in Mathematics (Springer-Verlag, Heidelberg, 1988), Vol. 1402, p. 69.
17. X.-D. Liu and S. Osher, Convex ENO high order schemes without field-by-field decomposition or staggered grids, *J. Comput. Phys*. **142**, 304 (1998).
18. W. Mulder, S. Osher, and J. A. Sethian, Computing interface motion in compressible gas dynamics, *J. Comput. Phys*. **100**, 209 (1992).
19. H. Nessyahu and E. Tadmor, Nonoscillatory central differencing for hyperbolic conservation laws, *J. Comput. Phys*. **87**, 408 (1990).
20. S. Osher and J. A. Sethian, Fronts propagating with curvature dependent speed: Algorithms based on Hamilton–Jacobi formulations, *J. Comput. Phys*. **79**, 121 (1988).
21. S. Osher and C. W. Shu, High order essentially non-oscillatory schemes for Hamilton–Jacobi equations, *SIAM J. Numer. Anal*. **28**, 902 (1991).
22. C. W. Shu and S. Osher, Efficient implementation of essentially non-oscillatory shock capturing schemes, II *J. Comput. Phys*. **83**, 32 (1989).